FORMING ANALYSIS OF CHOPPED FLAX FIBRE REINFORCED POLYPROPYLENE COMPOSITES

Wentian Wang[a*], Adrian Lowe[a], Shankar Kalyanasundaram[a]

[a]*Research School of Engineering, Australian National University, North Road, Canberra 0200, Australia*
**wentian.wang@anu.edu.au*

Keywords: Natural fibre reinforced composite, Stamp forming, Real-time strain measurement

Abstract
This work presents fundamental results on the research carried out by stamp forming of a chopped flax fibre reinforced polypropylene composite. The application of the real time non-contact strain measuring system, ARAMIS™, facilitates observations on material behaviour during forming. Through visual, microscopic and Scanning Electron Microscope (SEM) examinations, the major failure mode exhibited in the flax/polypropylene composite at room temperature is identified as fibre fracture. The punch load versus displacement curves at different blank holder forces are also analysed to determine the effect of blank holder force on the energy required for forming. The study of strain evolution at points of interest illustrates that blank holder force is a major factor in stamp forming of natural fibre reinforced composites. The results obtained in this study provide insight into challenges facing stamp forming of this class of material systems.

1. Introduction
Weight reduction can significantly contribute to reducing Green House Gas (GHG) emissions from vehicles. A 100kg weight reduction in a typical automobile leads to a reduction of 9 grams of CO_2-equivalent GHG emissions every kilometre travelled [1]. In addition to the significant increase in the demand on transportation due to the increase in global population, there is an urgent need to reduce the weight of vehicles to increase their fuel efficiency and therefore to reduce global GHG emissions. Driven by ecological and economic interests, there has been an increasing use of “green” or natural-fibre based material systems in various applications over the past decade. Flax fibre reinforced composite is a promising material system for use in automotive components due to its low weight, low cost, recyclability, and natural abundance [2-5].

The drawbacks in properties of natural fibres can also affect natural fibre reinforced polymer composites. The low thermal resistance of natural fibres causes possible degradation in mechanical properties at relatively low temperatures, which may limit the application of temperature on this material system [6]. Approximate 60% of natural fibres experience thermal degradation between 250˚ to 310˚ with an apparent activation energy of 160-170 kJ/mol [7]. In addition, the hydrophilic nature of natural fibres causes a weak bond with the composite matrices which are usually hydrophobic. Silva et al. [8] found that despite the great care taken during composite processing, entrapped air could not be entirely eliminated in the natural fibers/castor oil polyurethane composites and some bubbles were observed in the fracture surface morphology.

Failure modes in the fibre-reinforced composite include fibre/matrix debonding, fibre fracture, fibre pull out, matrix crack and delamination [9-10]. A number of studies have been carried out on analysing the major failure modes exhibited in fibre reinforced composites. Diansen et al. [11] explored the failure mechanisms exhibited in E-glass/TDE-85 epoxy resin braided composites in three point bending tests and he found that testing temperature had a visible impact on the damage of the composite. The composite exhibited a major failure mechanism of fibre fracture at room temperature, a combination of fibre fracture and cracks in matrix between 55˚-100˚ and a dominant failure mode of cracks in matrix at 120˚. Amit et al. [12] analysed the failure modes exhibited in a unidirectional carbon fiber tow composites compressed in different off-axis. The dominant failure mode changes from fibre tow buckling at small angles (15˚) to a combination of interfacial shear between tows and transverse compression at approximately 30˚-45˚.

Currently, the range of applications involved with natural fibre composites is still limited and one of the main challenges is a suitable mass production technique. Stamp forming is a rapid forming technique which has been widely used for forming metal panels in automotive industries. Forming natural fibre composites through stamp forming can be blended into the current tooling facilities used in automotive manufacturing factories, which lowers the operating costs of producing automotive parts for this class of material systems. A number of investigations have been carried out to analyse the forming capabilities of polypropylene (pp) composites with different fibre reinforcements in stamp forming [13-15]. The results obtained from these studies suggest that stamp forming is a feasible manufacturing technique for mass production of pre-consolidated fibre reinforced polypropylene composites. It was also found that a fibre-metal laminate (FML) structure based on a self-reinforced polypropylene composite is able to exhibit a superior formability when compared to monolithic metal alloys [1, 16-20].

This paper investigates the major failure mode exhibited in the chopped flax fibre reinforced polypropylene composite in stamp forming through visual, microscopic and SEM examinations. The effect of blank-holder force (BHF) on the forming behaviour of the composite is determined through analysing the punch load displacement curves and the strain evolutions at points of interest.

2. Experimental Setup

The material system used in this study consists of 50% weight of chopped flax fibres in a polypropylene matrix. The pre-consolidated composite is manufactured by EcoTechnilin, UK. All specimens are cut into a circle with a diameter of 180mm and are then formed into a dome structure to analyse two major forming modes encountered in stamp forming: drawing and stretching. The open die design of the press machine facilitates the application of a real-time non-contact strain measuring system, ARAMIS™, to capture the surface motion of the specimen during forming. The ARAMIS™ system then uses photogrammetric methodologies to compute surface displacement and strain deformation. In order to obtain the ideal condition for the ARAMIS™ system to capture surface motion of the specimen, samples are painted with a stochastic pattern of black dots on top of the white background to maximise the colour contrast of the surface. The measuring system is very accurate with less than 0.02% error in strain measurements. For the SEM examination, the facture surface was lightly platinum coated and examined through a Hitachi™ machine.

3. Results and discussion

3.1. Failure mechanism exhibited in the tested sample

In order to determine the failure mechanism exhibited in flax/pp composites, a microscopic examination was conducted in the failure region of the tested sample.

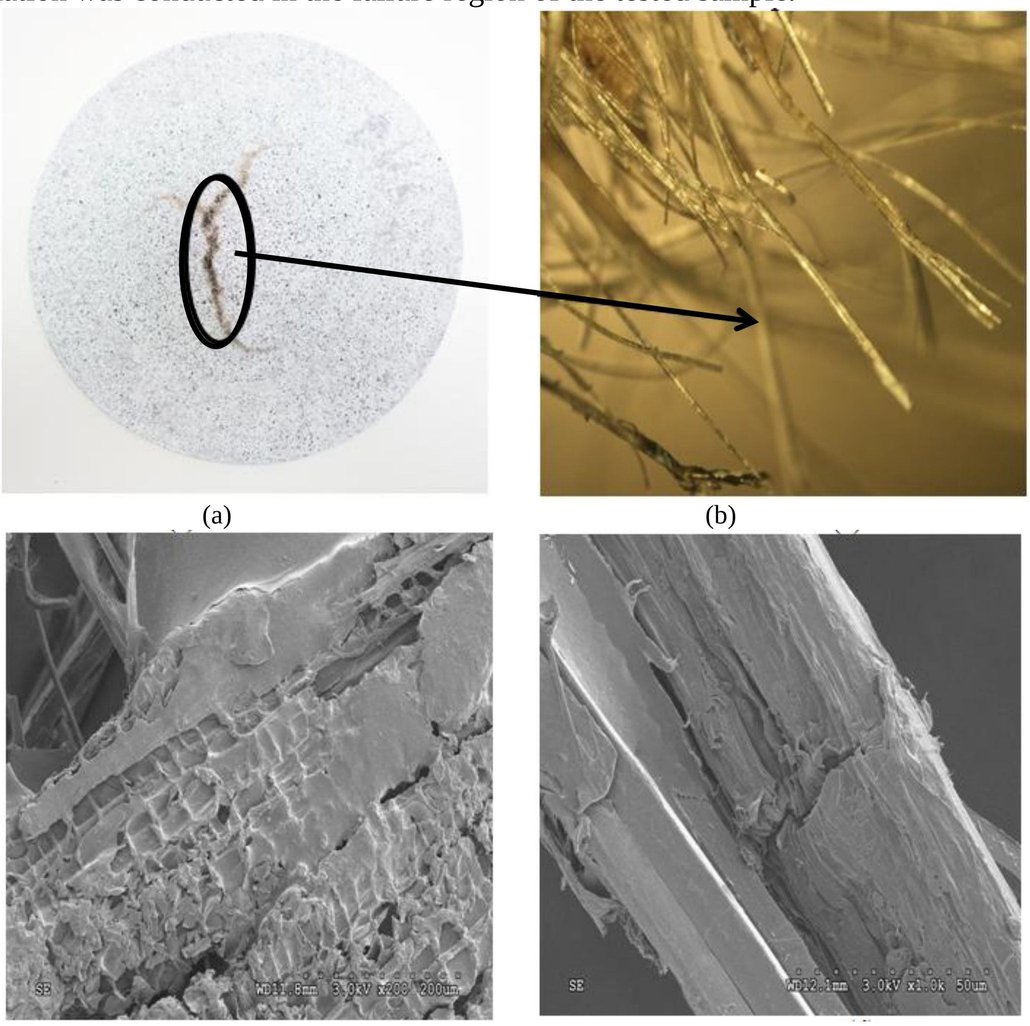

(a) (b) (c) (d)

Fig 1. Observation of a chopped flax/pp composite through (a): Visual examination, (b): Microscopic examination, (c): SEM examination on the fracture surface, (d): SEM examination on the flax fibre.

Figure 1a and 1b show a typical failure region exhibited in a tested sample and a microscopic image of the failure region, respectively. A significant amount of fractured fibres can be observed in the failure region of the composite. Flax fibres are short and randomly oriented in composites, and the failure region tends to propagate across the fibre rather than along the fibre due to lower value in strain to failure of the fibres compared to the polypropylene matrix. This contributes significantly to the irregular shape of the fracture exhibited in the composite. In addition, the failure region is mainly located around the centre of the specimen which experiences large strain deformations during forming. Clear evidence of fibre fracture can be found in the microscopic image of the failure region, suggesting that fibre fracture can be identified as the major failure mode for the chopped flax/pp composite in dome forming experiments.

According to figure 1c, some air bubbles can be observed, indicating the existence of entrapped air in the composite. This correlates well with the findings obtained by Silva et al [8]. The existence of air bubbles can also cause variations in the mechanical properties of the composite, leading to some regions being more strained than nearby regions and in turn resulting in possible early initiation of cracks. In figure 1d, the flax fibre is coated with polypropylene matrix indicating a relatively strong interface between flax fibres and the polypropylene matrix at failure. This is an indication that interfacial failure between flax fibres and the polypropylene matrix is not the major failure mode exhibited in the composite.

3.2 Effects of BHF on the punch load displacement curves

The area under the punch load versus displacement curves represents the amount of energy absorbed by specimens from toolings during forming, and the sudden drop in the punch load curve indicates the onset of crack initiation. During experiments, the punch was set to return to its original position when the punch load drops to 80% of the maximum load. This experimental setting helps analyse the post failure behaviour of the composite in dome forming experiments. According to figure 2, the chopped flax/pp composites exhibit a stable and slow drop in punch load after reaching the maximum load regardless of the magnitude of BHFs.

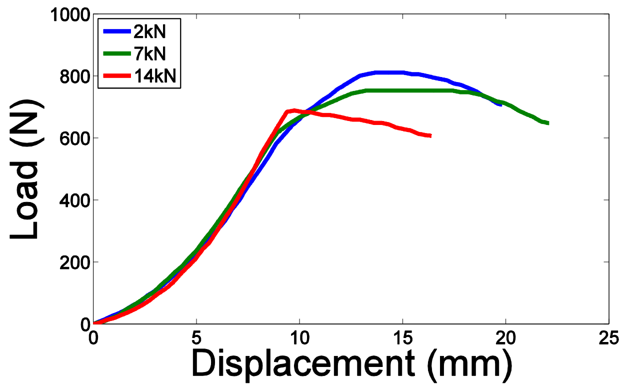

Fig 2. Effects of BHFs on the punch load versus displacement curves

Figure 2 also illustrates that at small BHFs (2kN and 7kN), punch loads continue to rise with a noticeably declined slope after forming to a depth of 10mm, indicating that the composite starts drawing into the die cavity. This evidence is not clearly observed for the composite formed at 14kN. The friction between the specimen and tools (the blank-holder and the die) increases with incresing BHF, and the composite needs to overcome the friction force exerted by tools when it draws into the die cavity. Therefore, less material draw is observed in the punch load curve obtained at a BHF of 14kN.

After the initiation of the crack at maximum load, the punch load experiences a plateau at small BHFs, especially at 7kN. For the experiment performed at large BHF (14kN), the composite behaves slightly different after the initiation of the failure compared to small BHFs. At 14kN BHF, the forming distance after the initiation of the failure is shorter with a lightly steeper slope, suggesting a smaller resistance to the propagation of cracks exhibited in the composite. The large BHF results in a larger stretch experienced by the composite, which accelerates the propagation of the crack.

To further analyse the post failure behaviour of the composite, two images from the left camera of the ARAMIS™ system at stages when the punch is at the maximum load and just about to detach from the specimen, respectively are illustrated in Figure 3.

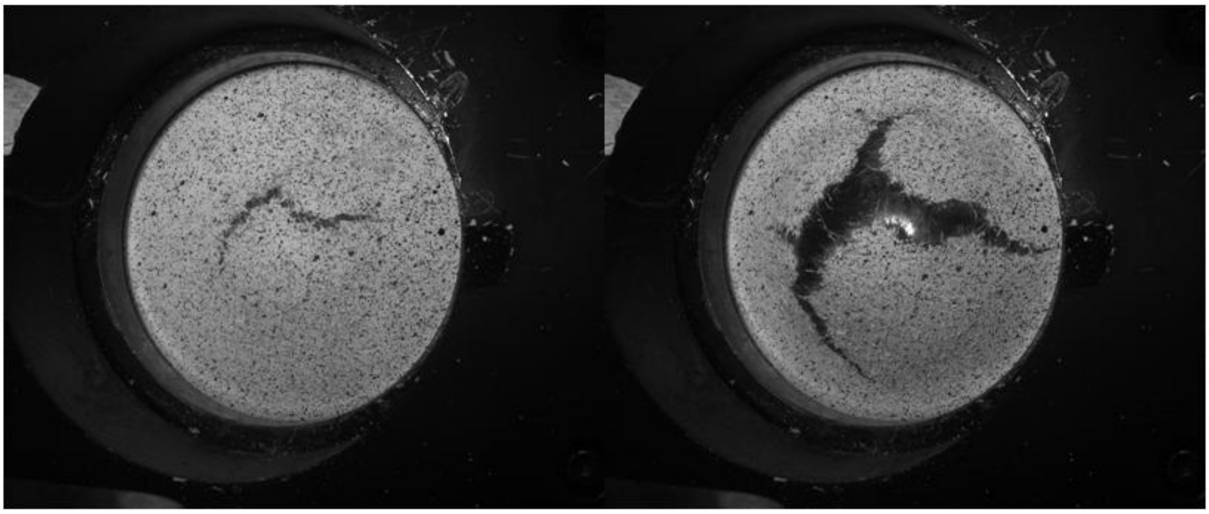

(a) (b)

Fig 3. Typical stage images captured by the left camera of the ARAMIS™ system when the punch is, a: at the maximum load, b: about to detach from the specimen

Figure 3 shows a significant expansion in the failure region between two stage images. The intial crack is confined in a small region around the pole which experiences the maximum strain deformation during forming. The larger failure strain in the ductile polypropylene matrix compared to flax fibres helps confine the failure region in a small area around the pole at the initiation of cracks. The major crack expands to a larger area when the composite is continued to be formed after failure, and there is no evidence of new cracks in the composite surface. This post failure behaviour of the composite explains the stable and slow drop in punch loads.

3.3 Effects of BHF on strain evolution at regions of interest

The chopped flax/pp composites predominantly exhibit isotropic material behaviour due to the random distribution of flax fibres. Therefore, an investigation on the strain evolution is conducted at two different surface points to analyse the major forming modes exhibited in the composite during dome forming, biaxial stretch and plane strain. Point A which is located at the pole of the specimen exhibit biaxial stretch during forming. Point B is located 40mm away from the pole in the horizontal axis and it exhibit plane strain conditions. At each point of interest, the evolution of major strain, strain in horizontal axis (ε_X), strain in vertical axis (ε_Y) and strain in shear directions (ε_{XY}) are plotted and compared to determine the effect of BHF on the forming behaviour of flax/pp composites in stamp forming.

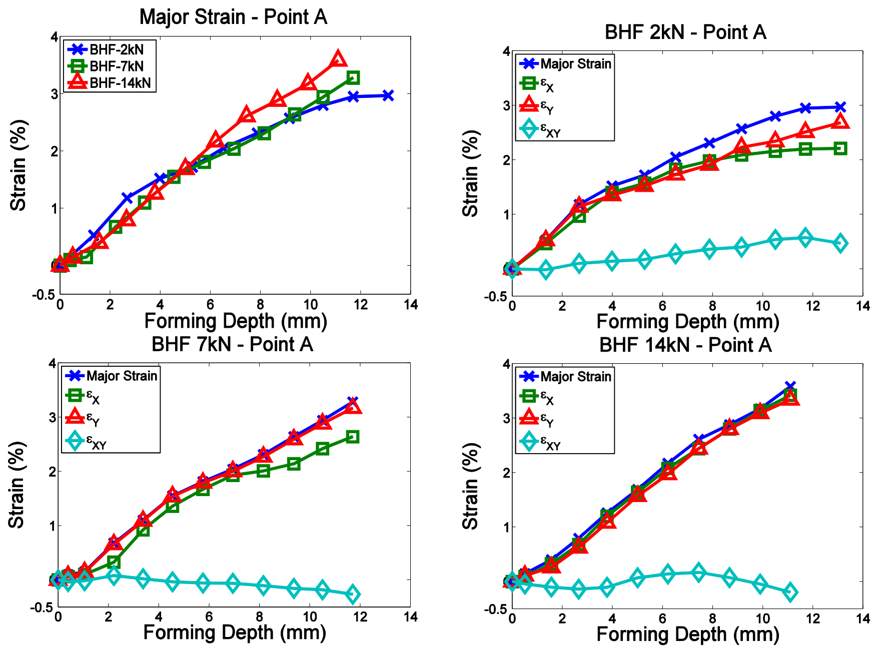

Fig 4. Strain evolutions at Point A under different BHFs

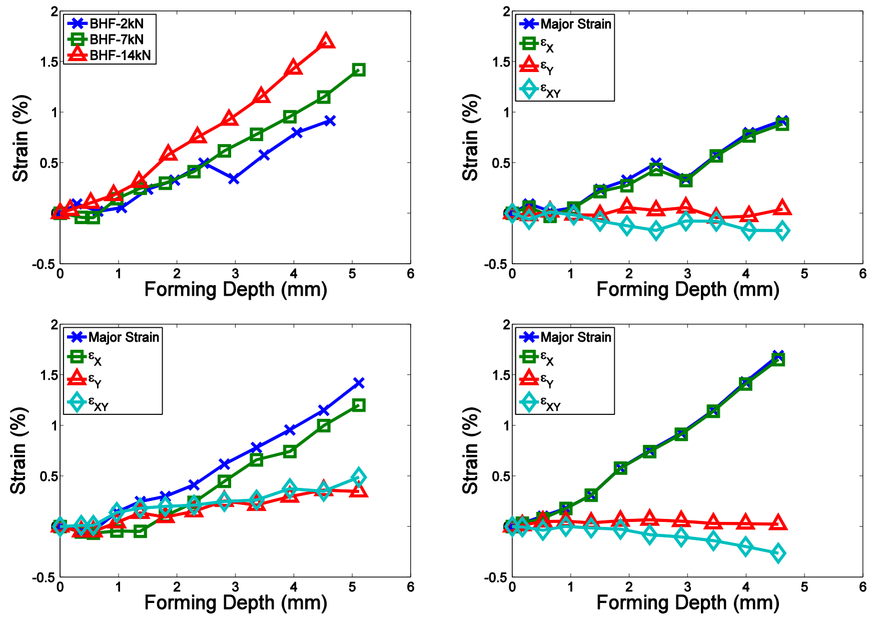

Fig 5. Strain evolutions at Point B under different BHFs

By comparing figure 4 and 5, the pole of the composite experiences a larger major strain compared to the unsupported edge during the entire strain evolution, indicating that strain deformation was confined within the central area of the composite. This correlates well with the finding obtained in previous sections that the major crack initiates around the pole of the specimen. Fibre fracture is the major failure mechanism exhibited in the composite, and the flax fibres which are mostly strained tend to be fractured early.

Figure 4 shows that the major strain at pole is governed by the strain in ε_X and ε_Y. This indicates that pole experiences a major forming mode of biaxial stretch during forming. Major strain at a BHF of 2kN levels out at large forming depths and similar trends cannot be clearly identified at other BHFs. This observation suggests that the composite starts drawing into the die cavity at large forming depths when the material flow is not sufficiently resitrcited at small BHF. Interestingly, the strain evolutions of ε_X and ε_Y are almost identical with negligible ε_{XY} when the specimen is formed at a BHF of 14kN, suggesting a forming mode close to balanced biaxial stretch. The pole of the specimen tends to experience a forming mode closer to the balanced biaxial stretch when the material flow is fully restricted at large BHF.

Figure 5 illustrates the effect of BHF on strain evolution at Point B. The major strain at this point is dominated by the strain in the horizontal axis, suggesting a major forming mode of plane strain. Similar to point A, the major strain of point B levels out at large forming depths at small BHFs. This further validates that the composite starts drawing into the die cavity at large forming depths when the material flow is insufficiently restricted. The specimen experiences more stretch, and therefore a larger strain deformation at unsupported regions at large BHFs. The maximum major strain rises by 42% from 0.91% at a BHF of 2kN to 1.42% at a BHF of 7kN, and increases further by 13% to 1.69% at 14kN BHF. It is also observed that point B experiences negligible ε_Y and ε_{XY} at a BHF of 14kN. Similar to point A, point B exhibits a forming mode closer to plane strain when the material flow is fully restricted at 14kN.

4. Conclusion

In stamp forming of chopped flax fibre reinforced polypropylene composite, the failure mode exhibited in the composite at room temperature is identified as fibre fracture through visual, microscopic and SEM examinations. Air bubbles are also observed in the specimen, causing variations in mechanical properties within the composite and possibly lead to early initiation of cracks in local regions. Observations on the post failure behaviour of the chopped flax/pp composite indicate that the composite exhibits a stable and slow drop in punch load due to the presence of randomly distributed short flax fibres and the ductility of the polypropylene matrix. The strain deformation is confined in the central area of the composite during forming. The unsupported edge of the specimen experiences an increased strain deformation wtih increasing BHF as the composite tends to experience more stretch and less draw at large BHF. When the material flow is fully rsetricted at a BHF of 14kN, points A (the pole) and B (40mm away from the pole in the horizontal axis) exhibit forming modes closer to biaxial stretch and plane strain, respectively. These experimental findings establish a foundation of the forming behaviour of natural fibre composites in dome forming.

Reference

[1] A. Sexton, W. Cantwell, MJ. Cardew-Hall, P. Compston, S. Kalyanasundaram. Stretch forming studies on a fibre metal laminate based on a self-reinforcing polypropylene composite, *Composite Structures,* 94: 431–437, 2012.
[2] PV. Joseph, K. Joseph, S. Thomas. Effect of processing variables on the mechanical properties of sisal-fibre-reinforced polypropylene composites, *Composites Science and Technology*, 59:1625-1640, 1999.
[3] P. Ouagne, D. Soulat, G. Hivet, S. Allaoui, D. Duriatti. Analysis of defects during the performing of a woven flax reinforcement, *Advanced Composites Letters* 20:97-100, 2011.
[4] C Baley. Analysis of the flax fibres tensile behaviour and analysis of the tensile stiffness increase. *Composite Part A*. 33:939–948, 2002.
[5] ZN. Azwa, BF. Yousif, AC. Manalo, W. Karunasena. A review on the degradability of polymeric composites based on natural fibres, *Materials and Design* 47:424-442, 2013.

[6] NM. Sergio, C. Veronica, JSR. Ruben, MM. Frederico. Thermogravimetric behavior of natural fibers reinforced polymer composites—An overview, *Materials Science and Engineering: A*, 557,17-28,2012.

[7] Y. Fei, W. Qinglin, L. Yong, G. Weihong, X. Yanjun. Thermal decomposition kinetics of natural fibers: Activation energy with dynamic thermogravimetric analysis. *Polymer Degradation and Stability*, 93,90-98,2008.

[8] RV. Silva, D. Spinelli, WW. Bose Filho, S. Claro Neto, GO. Chierice, J.R. Tarpani, Fracture toughness of natural fibers/castor oil polyurethane composites, *Composites Science and Technology*, 66, 1328–1335, 2006.

[9] AA. Fotouh, JD. Wolodko, MG. Lipsett, Fatigue Of Natural Fiber Thermoplastic Composites, *Composites: Part B* (2014), doi: http://dx.doi.org/10.1016/j.compositesb.2014.02.023

[10] WJ. Cantwell, J. Morton. The impact resistance of composite materials — a review, *Composites* 22/5,347-362,1991.

[11] L. Diansen, F. Daining, Z. Guobing, H. Hong, Effect of temperature on bending properties and failure mechanism of three-dimensional braided composite, *Materials and Design*, 41,167-170,2012.

[12] GS. Amit, MW. Anthony, C. Ari, Specimen size effects in the off-axis compression test of unidirectional carbon fiber tow composites, *Composites Science and Technology*, 64,83–89,2004.

[13] S. Kalyanasundaram, S. DharMalingam, S. Venkatesan, A. Sexton. Effect of process parameters during forming of self-reinforced – PP based Fibre Metal Laminate, *Composite Structures*, 97: 332-337, 2013.

[14] W. Wang, A. Lowe, S. Kalyanasundaram. A study on continuous flax fibre reinforced polypropylene composite in stamp forming process. *Advanced Composites Letters*, 22:86-89, 2013.

[15] S. Davey, R. Das, WJ. Cantwell, S. Kalyanasundaram. Forming studies of carbon fibre composite sheets in dome forming processes, *Composite Structures*, 97;310–316, 2013.

[16] L. Mosse, P. Compston, WJ. Cantwell, M. Cardew-Hall, S. Kalyanasundaram. Stamp forming of polypropylene based fibre–metal laminates: The effect of process variables on formability, *Journal of Materials Processing Technology*, 172: 163–168, 2006.

[17] L. Mosse, P. Compston, WJ. Cantwell, M Cardew-Hall, S. Kalyanasundaram. The effect of process temperature on the formability of polypropylene based fibre–metal laminates, *Composites Part A: Applied Science and Manufacturing*, 36;1158–1166, 2005.

[18] J. Gresham, WJ. Cantwell, M. Cardew-Hall, P. Compston, S. Kalyanasundaram. Drawing behaviour of metal–composite sandwich structures, *Composite Structures* 75;305–312, 2006.

[19] P Compston, WJ Cantwell, MJ Cardew-Hall, S Kalyanasundaram, L Mosse. Comparison of surface strain for stamp formed aluminium and an aluminium polypropylene laminate, *Journal of materials science*, 39;6087-6088, 2004.

[20] L Mosse, P Compston, WJ Cantwell, M Cardew-Hall, S Kalyanasundaram. The development of a finite element model for simulating the stamp forming of fibre-metal laminates, *Composite Structures*, 75;298-304, 2006.